Appendix C: Mathematical model developed for two particular cases of in-plane measurements.

The lack of information concerning the direction of the applied magnetic field H_{IP} with respect to the NWs direction in the IP plan (i.e. the easy IP directions) raises some additional complications to the mathematical modelling of the IP measurements. If one considers a NW with its axis making an angle α_i in the range $-\alpha_{max} \leq \alpha_i \leq \alpha_{max}$ with respect to the OOP direction and an azimuthal angle β_i with the IP direction of measurements, the NW axis makes an angle θ_i with the IP direction of measurements, as depicted in Figure 76. The angle θ_i is given, in function of α_i and β_i, as

$$\cos(\theta_i) = \sin(\alpha_i)\cos(\beta_i) \tag{97}$$

This derivation is provided in Appendix D.

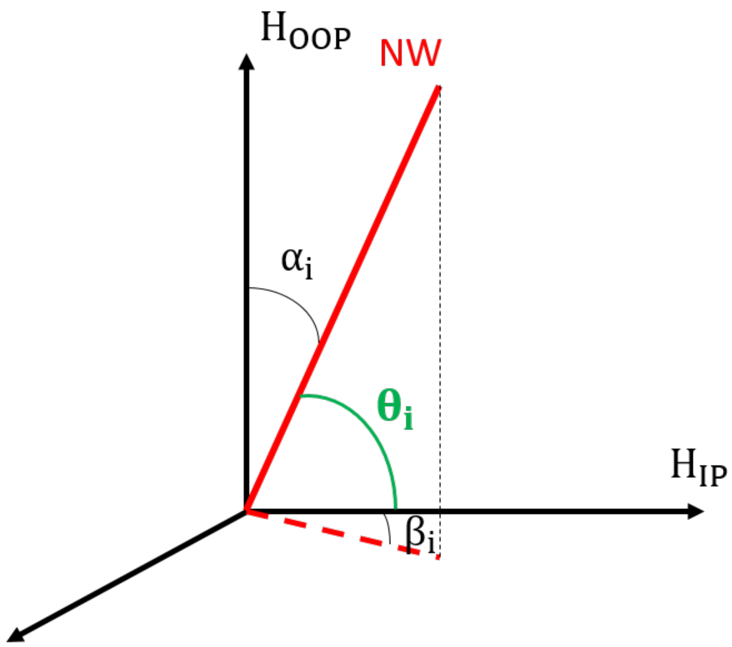

Figure 76: Schematic 3D representation of one NW of the networks that makes an angle α_i with the direction of H_{OOP} and an azimuthal angle β_i with the direction of H_{IP} resulting in an angle θ_i with the H_{IP} direction.

Figure 77 presents the measuring configuration. The applied field can either be applied in the OOP direction or in the IP direction perpendicular to the global current flow (See Subsection 2.3). Note that angular rotation of the applied field direction in the IP plane has been performed. The results are presented in the Appendix E. The angle β_i is *a priori* not known and can vary from one NW to another due to the standard angle deviation.

To simplify the equations, two particular cases, mathematically presented in Figure 78, will be considered:

- Case A: The magnetic field is increased along one of the IP easy direction. No net current crosses the NWs perpendicular to the global current flow. The current only flows along one NWs population.

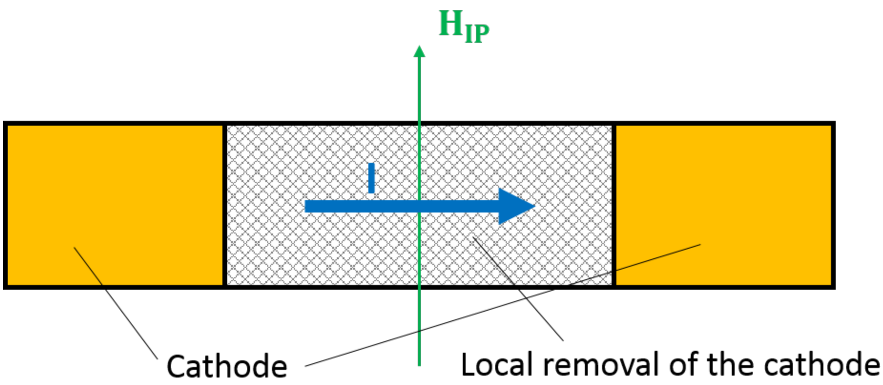

Figure 77: Schematic representation of the IP measuring configuration considered. The applied field is increased perpendicular to the global current flow.

- Case B: The magnetic field direction makes an angle of $\frac{\pi}{4}$ with both IP easy directions. The current is equally distributed along the two NWs populations. Therefore, the two NWs populations give an equal and identical contribution to the AMR effect.

Note that intermediary situations may be expected and raise the difficulty of the current division determination at the interconnections.

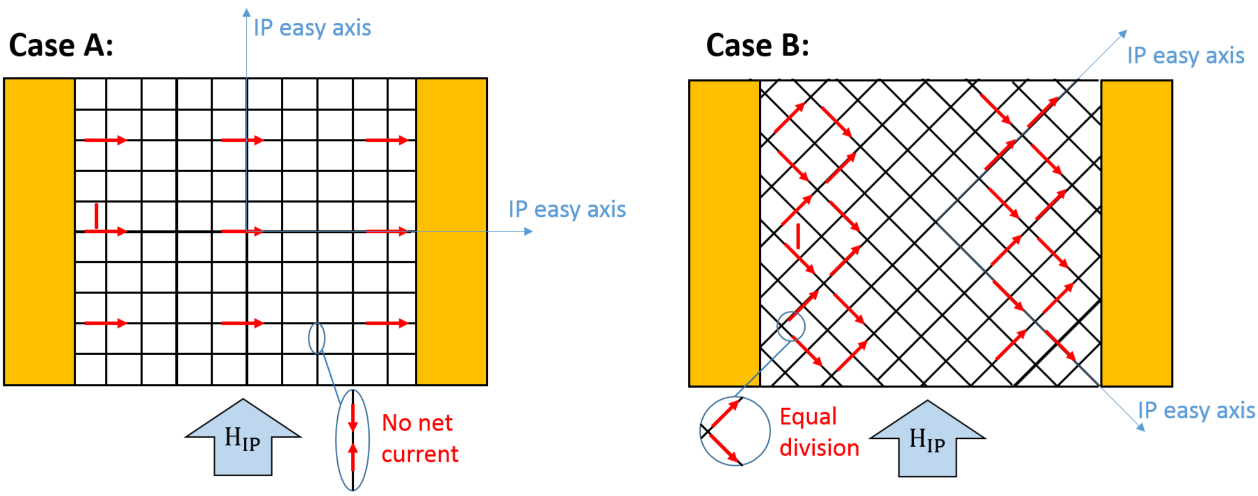

Figure 78: Schematic representation of the IP measuring configuration considered. The applied field is increased perpendicular to the global current flow.

The case A will be first considered. In this special case, when the magnetisation is saturated in the IP direction, the lower resistance $\rho_{\perp}^{IP}$ is reached, neglecting the interconnections contribution. Indeed, the current only crosses the NWs parallel to the global current flow and, thus, perpendicular to the applied magnetic field. Therefore, assuming that the saturation field is reached and that the higher resistive state is obtained at $H = 0$, one can easily derive the AMR ratio of the sample:

$$AMR_A^{IP} = \frac{\rho_{\parallel} - \rho_{\perp}^{IP}}{\rho_{av}^{IP}} \tag{98}$$

Which can be written as:

$$AMR_A^{IP} = \frac{1 - \frac{\rho_\perp^{IP}}{\rho_\parallel}}{\frac{1}{3} + \frac{2}{3}\frac{\rho_\perp^{IP}}{\rho_\parallel}} \tag{99}$$

This equation approximates the AMR effect using only the measurement of the normalised resistivity reached at $H_{IP} = \pm 10$ kOe. However, this situation is quite unlikely. The second limit case may present a more likely situation.

If one considers the case B, when the magnetisation is saturated in the IP direction, a resistive state $\bar{\rho}_{IP}$ higher than $\rho_\perp$ is reached. The AMR contribution of each NWs that makes an angle θ_i with the IP direction is given by:

$$\rho(\theta_i) = \rho_\perp + (\rho_\parallel - \rho_\perp)\cos^2(\theta_i) \tag{100}$$

Averaging this equation with $0 \leq \alpha_i \leq \alpha_{max}$ and $\beta = \frac{\pi}{4}$ is equivalent to averaging the equation with $\theta_m \leq \theta_i \leq \frac{\pi}{2}$. Using the equation 97. One gets:

$$\cos\theta_m = \sin(\alpha_{max})\cos(\beta) = \frac{1}{\sqrt{2}}\sin(\alpha_{max}) \tag{101}$$

Therefore, one has:

$$\bar{\rho}_{IP} = \frac{1}{\frac{\pi}{2} - \theta_m}\int_{\theta_m}^{\frac{\pi}{2}} \rho_\perp + (\rho_\parallel - \rho_\perp)\cos^2(\theta)\ \ \mathrm{d}\theta \tag{102}$$

The integration provides:

$$\bar{\rho}_{IP} = K_-^{IP}\rho_\parallel + K_+^{IP}\rho_\perp \tag{103}$$

With:

$$K_\pm^{IP} = \frac{1}{2} \pm \frac{1}{4(\frac{\pi}{2} - \theta_m)}\sin(2\beta_m) \tag{104}$$

$K_\pm$ only depend on the angle θ_m and obey to the relation:

$$K_+^{IP} + K_-^{IP} = 1 \tag{105}$$

Assuming that $\bar{\rho}_{IP}$ is reached, one can derive the unknown lower resistive state of the sample $\rho_\perp^{IP}$ from Equation 103:

$$\rho_\perp^{IP} = \frac{1}{K_+^{IP}}(\bar{\rho}_{IP} - K_-^{IP}\rho_\parallel) \tag{106}$$

That can be written as:

$$\frac{\rho_\perp^{IP}}{\rho_\parallel} = \frac{1}{K_+^{IP}}(\frac{\bar{\rho}_{IP}}{\rho_\parallel} - K_-^{IP}) \tag{107}$$

With $\frac{\bar{\rho}_{IP}}{\rho_\parallel}$ being the normalised resistivity reached at $H_{IP} = \pm 10$ kOe, assuming that the magnetisation is saturated.

As the higher resistive state is supposed to be obtained at $H = 0$, on can get the AMR ratio:

$$AMR_B^{IP} = \frac{\rho_\parallel - \rho_\perp^{IP}}{\rho_{av}^{IP}} \tag{108}$$

Which can be written as:

$$AMR_B^{IP} = \frac{1 - \frac{\rho_\perp^{IP}}{\rho_\parallel}}{\frac{1}{3} + \frac{2}{3}\frac{\rho_\perp^{IP}}{\rho_\parallel}} \tag{109}$$

This equation approximates the AMR effect using only the measurement of $\frac{\bar{\rho}_{IP}}{\rho_\parallel}$, the normalised resistivity reached at $H_{IP} = \pm 10$ kOe. The decrease of resistance being more important when measuring in the IP direction, compared with the OOP measurements, the AMR calculation error is expected to be smaller using IP measurements. However, the lack of information about the IP direction yields a new source of error.

The calculation of the AMR ratio can be done using $\bar{\rho}_{OOP}$ or $\bar{\rho}_{IP}$. As both measurement have been done, one can verify the validity of the model. Indeed, as the configuration where the magnetisation is perpendicular to the NWs axis is independent of the direction of the magnetic field, one expects that $\rho_\perp^{OOP}$ and $\rho_\perp^{IP}$ are equal. This yields, in the case A:

$$\bar{\rho}_{IP} = \frac{1}{K_-^{OOP}}(\bar{\rho}_{OOP} - K_+^{OOP}\rho_\parallel) \tag{110}$$

And thus:

$$\frac{\bar{\rho}_{IP}}{\rho_\parallel} = \frac{1}{K_-^{OOP}}(\frac{\bar{\rho}_{OOP}}{\rho_\parallel} - K_+^{OOP}) \tag{111}$$

And in the case B:

$$\frac{1}{K_+^{IP}}(\bar{\rho}_{IP} - K_-^{IP}\rho_\parallel) = \frac{1}{K_-^{OOP}}(\bar{\rho}_{OOP} - K_+^{OOP}\rho_\parallel) \tag{112}$$

Which provides:

$$\bar{\rho}_{IP} = \frac{K_+^{IP}}{K_-^{OOP}}\bar{\rho}_{OOP} + \frac{1}{K_-^{OOP}}(K_-^{OOP}K_-^{IP} - K_+^{OOP}K_+^{IP})\rho_\parallel \tag{113}$$

And thus:

$$\frac{\bar{\rho}_{IP}}{\rho_\parallel} = \frac{K_+^{IP}}{K_-^{OOP}}\frac{\bar{\rho}_{OOP}}{\rho_\parallel} + \frac{1}{K_-^{OOP}}(K_-^{OOP}K_-^{IP} - K_+^{OOP}K_+^{IP}) \tag{114}$$

The maximal angle between the NWs and the OOP direction is $\alpha_{max} = \frac{\pi}{4}$. Therefore, the maximal angle between the NWs and the IP direction is $\theta_m = \text{acos}(\frac{1}{2}) = \frac{pi}{3}$. Using those results, one gets:

$$K_\pm^{OOP} = \frac{1}{2} \pm \frac{1}{\pi}\sin(\frac{pi}{2}) = \frac{1}{2} \pm \frac{1}{\pi} \tag{115}$$

And:

$$K_\pm^{IP} = \frac{1}{2} \pm \frac{1}{4(\frac{\pi}{2} - \frac{pi}{3})}\sin(2\frac{pi}{3}) = \frac{1}{2} \pm \frac{1}{2\frac{\pi}{3}}\frac{\sqrt{3}}{2} = \frac{1}{2} \pm \frac{3\sqrt{3}}{4\pi} \tag{116}$$

Figure 79 presents the two models for the case A (blue) and the case B (red), with α_{max} =45°. The blue and red shaded area represents the calculated models in the range 40°-50°, to take into account the effect of the standard angle deviation of ±5°. One can observe that the models are quite close. It can be supposed that intermediary configurations lead to intermediate results. However, it may be more complex.

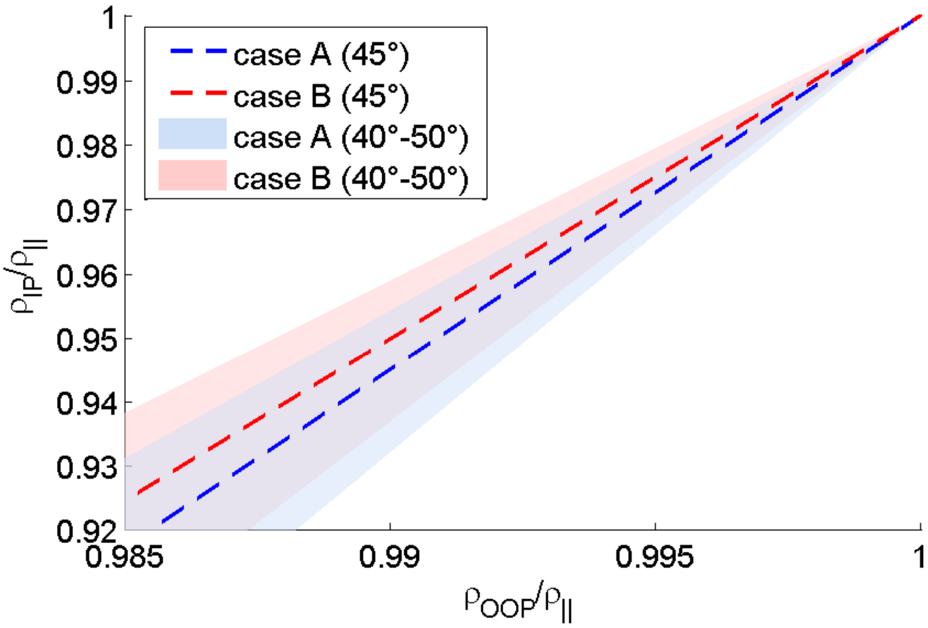

Figure 79: Mathematical relation between $\frac{\bar{\rho}_{IP}}{\rho_{\|}}$ and $\frac{\bar{\rho}_{OOP}}{\rho_{\|}}$ for the case A (blue) and B (red) with α_{max} =45°. The blue and red shaded area represents the calculated models in the range 40°-50°, to take into account the effect of the standard angle deviation of ±5°.